Tracking Studies with Frequency Ramp for the APS-U Booster

Andi Gu
Mentors: Uli Wienands, Joe Calvey

August 7, 2020

Contents

Abstract

One of the primary goals for the proposed Advanced Photon Source upgrade (APS-U) is to improve the quality and intensity of the storage ring's synchrotron radiation output. To achieve this, it is necessary for the booster to deliver a large bunch charge at once – where the current charge ceiling for a single bunch is 6nC, the booster must now be able to reliably deliver > 17nC for the APS-U. This requires the introduction of a time-varying radio frequency (RF) into the booster ring RF cavities. This report will discuss the effects of the frequency ramp, along with other relevant RF cavity parameters. We study these effects using the `elegant` simulation program, and explore various techniques that may be employed to achieve desirable beam characteristics. More specifically, the two characteristics we will discuss are efficiency at high charge, and horizontal emittance at extraction. We present the simulations results and their implications for the APS-U.

1 Introduction

Synchrotron radiation, a form of highly collimated light produced when electrons are accelerated radially, has applications in a broad spectrum of scientific fields, ranging from medical imaging to materials engineering. It is so useful, in fact, that this form of radiation is the primary product of Argonne National Lab's Advanced Photon Source (APS). One of the characteristics of this radiation that makes it especially effective for scientific applications is its brightness, and it is expected that increases in the APS synchrotron radiation brightness will enable novel applications in basic science and applied research. The proposed APS upgrade (APS-U) plans to achieve this increased brightness in part by ensuring new components have the ability to deliver high charge to the storage ring.

To achieve this target, each stage of the beam line must meet certain functional requirements. In particular, the booster ring's function is to accelerate a low energy beam from the particle accumulator ring (PAR) to high energies expected by the storage ring. This is an acceleration from around 450MeV to 6GeV in just under 0.2s.

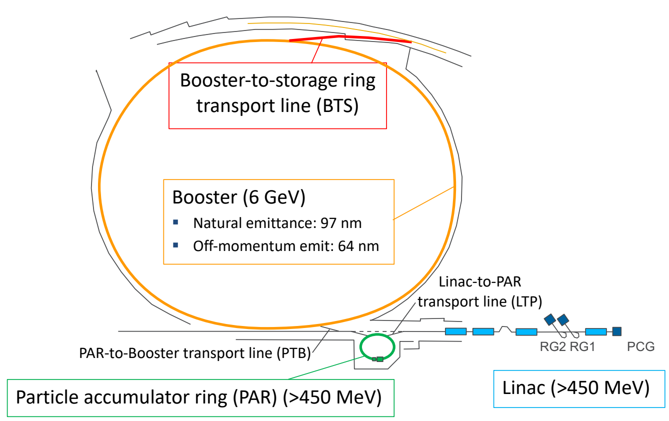

Figure 1: A schematic of the APS-U injector complex[1]

[1]Courtesy: K. Harkay

Beyond this basic requirement, the booster must now achieve two additional benchmarks for the APS-U [1]:

(I) Reliably deliver a high charge (> 17nC) beam with an efficiency $> 85\%$.

(II) Ensure a horizontal beam emittance at extraction ϵ_x that meets storage ring requirements. For this study, it will be required to be below 60nm.

It proves difficult to achieve requirement (II) if the beam is run on-momentum at extraction. However, since the damping partition numbers J_x and J_z can be manipulated by running the beam off-momentum, we opt to extract the beam slightly off-momentum to increase damping in the horizontal plane (at the cost of decreased longitudinal damping). Therefore, the booster must be able to carry out an ‘offset ramp’, which smoothly varies the beam momentum offset δ_p from injection[2] to the the desired extraction offset. This necessitates the introduction of a corresponding frequency ramp: to control the momentum offset, the frequency of the booster cavities must be varied in time appropriately. On the other hand, requirement (I) has been studied [2, 3], however, the introduction of a frequency ramp is novel and its effects must be studied. This report will discuss the effects of this frequency ramp, and whether it is useful in achieving (I) and (II).

Despite some hard restrictions, such as the momentum offset at extraction, there are several free parameters that remain in the booster, such as initial momentum offset, cavity detuning, and features of the cavity voltage ramp. This study will use the `elegant` simulation program[3] to understand each of these parameters and their effects, as well as the effects of a frequency ramp.

2 Ramp Calculations

We intend to inject the beam into the booster lattice at 425MeV and some momentum offset $-0.003 \leq \delta_{p,0} \leq -0.007$, then extract the beam at 6GeV and momentum offset $\delta_{p,ex} = -0.008$. To achieve this while ensuring a stable beam, we must calculate an appropriate frequency, phase, and voltage ramp.

2.1 RF Cavity Frequency

To maintain an arbitrary momentum offset δ_p, the RF cavity must be driven with a frequency $f = \frac{c}{C_{booster}(1+\delta_p \eta)}$ (or some integer multiple thereof)[4]. For a relativistic beam $\eta \approx \alpha_c$, and we can Taylor expand to the first order to find

$$f_{booster} = h_{booster} \frac{c}{C_{booster}} (1 - \delta_p \alpha_c) \tag{1}$$

However, to ensure bucket alignment is achievable, we impose an additional restriction that $f_{booster}$ must be some rational multiple of the storage ring frequency f_{SR} – more specifically, that at injection and extraction

$$f_{booster} = f_{SR} \left(1 - \frac{1}{N}\right) \quad \text{for some integer } N \tag{2}$$

[2]Although it turns out injecting off-momentum has adverse effects, it is necessary to do so due to practical limitations discussed in §4.1.1.

[3]`elegant` is a simulation program developed at Argonne for tracking beams through accelerator models.

Since the analytical relationship in equation (1) cannot always satisfy restriction (2), we must replace injection and extraction momentum offsets with values that have been tweaked up or down as necessary.

Under the formulation of (2), we use a function $m(t)$ to characterize the frequency ramp: $f_{booster} = f_{SR}\left(1 - \frac{m(t)}{N_1 N_2}\right)$, with the requirement that $m(t_0) = N_2$ and $m(t_1) = N_1$. For $t_0 < t < t_1$, we opt to use a cossine ramp, so that $m(t)$ can be defined piecewise as follows[4]:

$$m(t) = \begin{cases} N_2 & \text{for } t \leq t_0 \\ N_2 + \frac{N_1 - N_2}{2}\left(1 - \cos\left(\frac{\pi(t-t_0)}{t_1 - t_0}\right)\right) & \text{for } t_0 < t < t_1 \\ N_2 & \text{for } t \geq t_1 \end{cases} \tag{3}$$

Figure 2a shows sample frequency ramps for a range of different initial momentum offsets.

2.2 Voltage Ramp

We are restricted by hardware limits on the voltage that is practically achievable inside the RF cavity. For this study, the maximum achievable voltage was taken to be 5.2MV [5]. Furthermore, we opt to use a quartic voltage ramp, since synchrotron losses (which dominate at high energies) are themselves also quartic. More specifically, we take our voltage ramp to be $V(t) = V_0 + b \cdot E(t)^4$, subject to the constraint that $V(t_1) = 5.2$MV. This leaves one free parameter in the voltage ramp: initial voltage V_0. This problem has been studied before [6], however, adding a frequency ramp on top of a voltage ramp cannot be assumed to result simply in a superposition of the two effects taken individually. Thus, V_0 is the subject of optimizations that are discussed later in this report.

2.3 Synchronous Phase

The booster RF cavity voltage must not only accelerate the beam to match the desired momentum ramp, but also to compensate for synchrotron radiation losses along the way. The necessary energy gain per turn is $\Delta U_{ramp} + \Delta U_{sync}$. Synchrotron loss per turn is $\Delta U_{sync}(\text{keV}) = 88.46 \frac{(U_{ref}(\text{GeV}))^4}{\rho(\text{m})}$, where ρ is the bending radius of the booster dipole magnets. In summary we have

$$\Delta U = \frac{\mathrm{d}U_{ref}}{\mathrm{d}t} \frac{C_{booster}}{c} + 88.46 \frac{(U_{ref})^4}{\rho} \tag{4}$$

To compensate for these two effects, we match the synchronous phase ψ_s to ΔU. Since the average energy gain per unit charge from the RF cavity is $V \sin \psi_s$, we simply calculate

$$\psi_s = \frac{\pi}{2} - \arcsin \frac{\Delta U(\text{MeV})}{V(\text{MV})} \tag{5}$$

The `elegant` program further requires a phase ramp, defined with

$$\phi(t) \equiv \psi_s(t) + \int_0^t f_{booster}(\tau)\, \mathrm{d}\tau \tag{6}$$

This ramp is determined solely by synchronous phase and frequency.

[4]In practice, a frequency correction term m_c is added to allow us to target specific buckets in the storage ring.

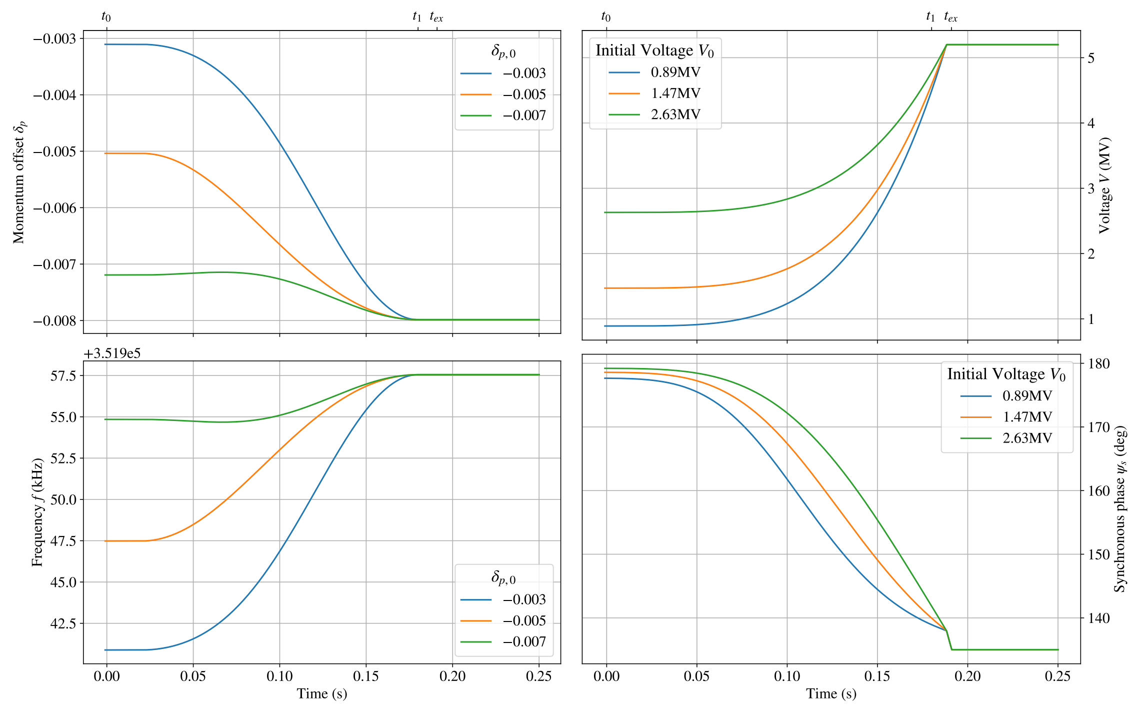

(a) Frequency ramp and momentum offset ramp

(b) Voltage ramp and synchronous phase ramp

Figure 2: Frequency and voltage ramps, with their corresponding momentum offset and synchronous phase ramps. The beam is injected at t_0, the frequency ramp ends at t_1, and the beam is extracted at t_{ex}.

3 elegant Simulation

The ramps are compiled into an `.sdds` file, and serve as the input for an `elegant` model that describes the proposed APS-U booster synchrotron.

3.1 Lattice Elements

We model the booster lattice as a singular matrix element via the `ILMATRIX` element, and track a beam of 5000 particles. This enabled a significant computational speed up, and made it practical to run many different parameter configurations in a reasonable amount of time. However, this model of the booster neglects some effects such as physical apertures, and therefore may slightly underestimate particle losses; to compensate for this, we impose a more stringent efficiency requirement of $> 90\%$ on simulation runs. Various elements are stacked on top of the `ILMATRIX` to represent other effects, enumerated below:

- `RFRAMP` as an RF cavity with a ramped voltage/frequency
- `RFMODE`, a resonator model with $\beta = 3$ that models the properties of the four booster RF cavities
- `SREFFECT` to account for synchrotron radiation losses
- `ZLONGIT` to account for longitudinal impedance
- `TCLEAN`, an aperture with a restriction $|\delta_p| \leq 0.025$ to model booster momentum acceptance

3.2 Running Simulations

There are four parameters whose effect we wish to understand:

1. Detuning Δf. Since the new RF cavities will have an increased coupling coefficient $\beta = 1 \to \beta = 3$, work must be done to understand their dynamics, especially at injection.
2. Initial momentum offset $\delta_{p,0}$.
3. Inital voltage V_0.
4. PAR bunch shortening. Increased longitudinal focusing in the PAR's 12th harmonic cavity can enable up to a 20% reduction in bunch length at injection.

Unless otherwise specified, we will understand that the parameters are set to the the reference configuration:

$$(\delta_{p,0}, \Delta f, V_0) = (-0.003, -2\text{kHz}, 1.47\text{MV}) \tag{7}$$

We run a search over these four parameters to determine the relative importance each may play in improving beam transmission and extraction emittances.

We simulate injecting beams of various charges, ranging from 1nC to 20nC. In light of the high charge requirement (I), we focus our attentions on injecting higher charges. The beam parameters at injection for various[5] bunch charges are first determined by collecting measurements from the PAR; they are listed in Table 1.

[5]For bunch charges not listed in the table, their parameters were found by linear interpolation between known injection parameters.

Table 1: Beam parameters at injection for various bunch charges

Charge Q_{bunch}	ϵ_x (nm rad)	ϵ_y (nm rad)	σ_s (cm)	σ_s (ps)	$\sigma_{s,80\%}$ (ps)	σ_p
1	253	27	9.8	325	260	0.00042
4	290	40	12.6	420	335	0.00044
8	340	70	14.4	480	385	0.00048
12	350	170	17.1	570	455	0.00047
16	370	250	21.0	700	560	0.00051
20	380	320	24.0	800	640	0.00051

NOTE – $\sigma_{s,80\%}$ represents the bunch length at 80% due to the increased longitudinal focusing in the PAR.

4 Results

It is known that the majority of the beam loss typically occurs at the low end of the momentum ramp. The results from `elegant` simulations are consistent with this observation (Figure 3). This is due to beam parameters being unmatched at injection; significant losses are incurred within the first few thousand turns. After these initial losses, the beam remains stable until the high end of the ramp, at which point voltage is unable to compensate for synchrotron losses (due to the imposed voltage limit). However, the losses due to this effect are negligible ($< 0.5\%$) compared to initial losses.

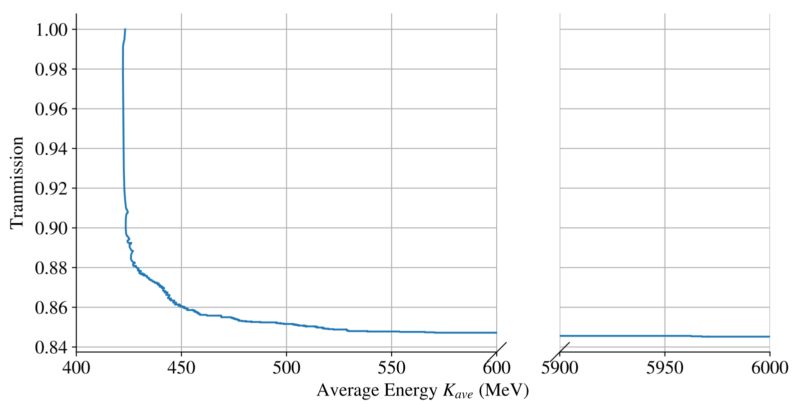

Figure 3: Fraction of particles remaining (transmission) vs. energy for $Q = 18$nC at reference configuration (7).

Due to this effect, it turns out that the transmission requirement (I) and emittance requirement (II) can be studied mostly separately of each other. To understand transmission, injection studies are sufficient, since losses past the first few thousand turns are largely negligible. On the other hand, to find extraction emittances, it is unavoidable that a full run to 6GeV must be done. However, we have the advantage that injection runs are relatively fast, and thus we can first determine a subset of booster parameters that satisfy the high charge requirement (I), and study only this smaller subset of parameter combinations for full runs.

4.1 Transmission

For the purposes of transmission studies, the runs were ended at 600MeV – after this point, losses were found to be negligible. Most of the effects discussed in the following section can be understood in terms of the relationship between bunch length and momentum spread (Figure 4).

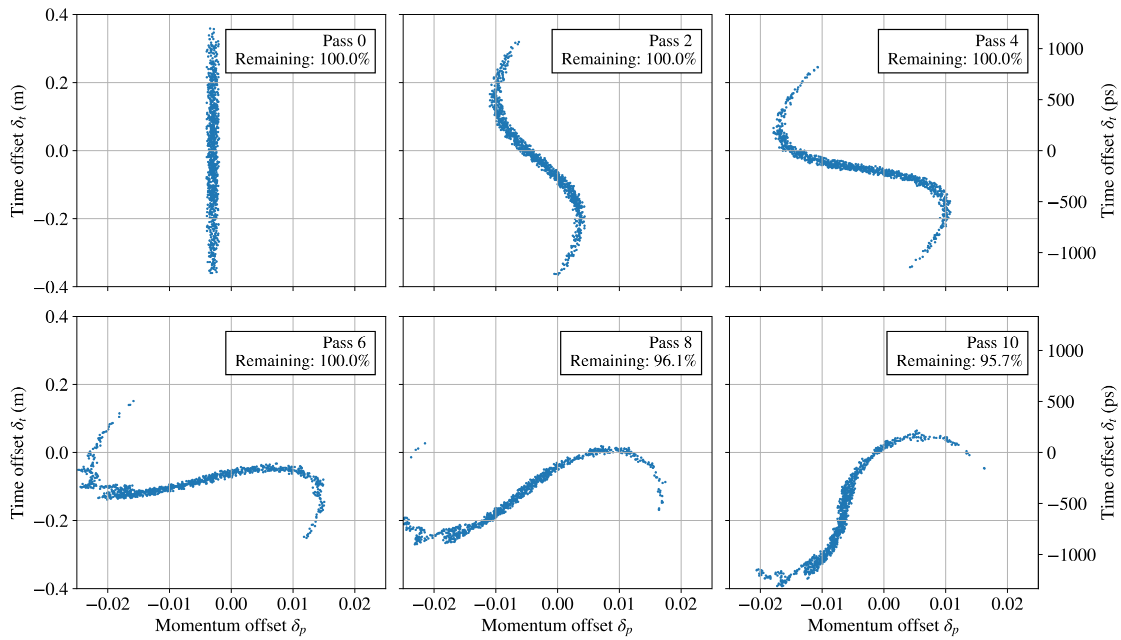

Figure 4: Phase diagrams for $Q_{bunch} = 18$nC, at the reference configuration (7). Momentum offset δ_p is plotted against longitudinal spread δ_t for every other turn. The nonlinear effects of the RF cavity voltage's sin waveform are evident in the growing 'S'-shape.

The event at pass 8 (approximately the half synchrotron period) explains most of the losses that occur at injection. A large initial bunch length (evidenced by the spread of δ_t) eventually translates to a large momentum spread, at which point particles will be lost due to the momentum acceptance of the booster. For the purposes of this study, they are marked lost at $\delta_p \leq -0.025$ by the `TCLEAN` element, as can be seen at pass 8. Each of the following subsections discuss the effect of the variation of a single parameter.

4.1.1 Initial Momentum Offset

A range of different initial momentum offsets $-0.007 \leq \delta_{p,0} \leq -0.003$ were tried. In light of the beam behavior seen in Figure 4, it is no surprise that running further off-momentum at injection has adverse effects for transmission. To the first order, a beam that is further off-momentum would simply result in the phase plots in Figure 4 being shifted further to the left. Since all losses occur from running too far below reference momentum (i.e. there are no losses due to $\delta_p \geq 0.025$), a shift to the left would result in a larger fraction of particles being lost simply due to the momentum

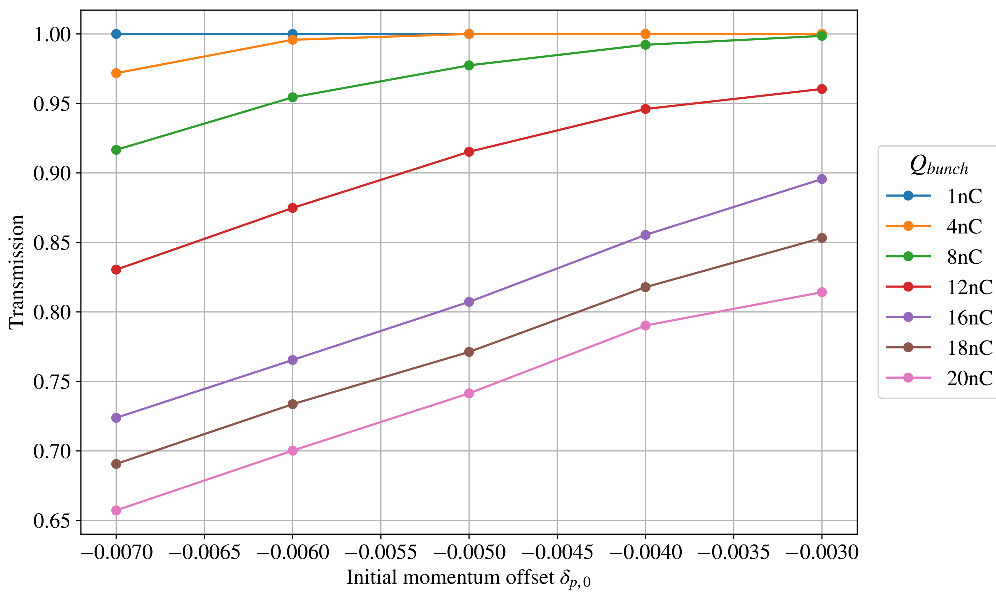

Figure 5: Transmission vs. initial momentum offset $\delta_{p,0}$

acceptance of the machine. There were no observed benefits (in terms of emittance or transmission) to injecting further off-momentum than necessary, and so $\delta_{p,0} = -0.003$ was found to be sufficient. This is as close as we can get to running on-momentum at injection – there is a limit of 0.5% on the total amount the momentum offset can change over the course of the frequency ramp, because a larger change would overstress on cavity couplers. Since we wish to extract at $\delta_{p,ex} = -0.008$, we can expect to inject with at most $\delta_{p,0} = -0.003$.

4.1.2 Initial Voltage

Although all voltage ramps behave fairly similarly towards the high end of momentum ramp, their behavior at the low end proves to be crucial. There are two competing effects at injection: the booster momentum acceptance and beam loading, which becomes non-negligible at higher bunch charges. A voltage that is too low will result in beam loading dominating the RF cavity; on the other hand, if the voltage is too high, although it may shorten the beam length, it will cause the momentum spread to grow too large. Clearly there is a balance to be achieved. The need for this balance is borne out by simulation results, as seen in Figure 6.

Simulations results suggest that there is a global optimum for initial voltage V_0, *regardless* of bunch charge, that lies in the neighbourhood of 1.47MV. Furthermore, tuning the initial voltage V_0 can have large benefits, especially at high charge: a difference in just 0.5MV can bring about an upwards of 10% change in transmission. However, this optimum seems to be fairly impervious to small errors: voltages in the window (1.47 ± 0.1)MV show negligible differences in transmission, and thus adjustments to cavity voltage do not need to be too fine tuned.

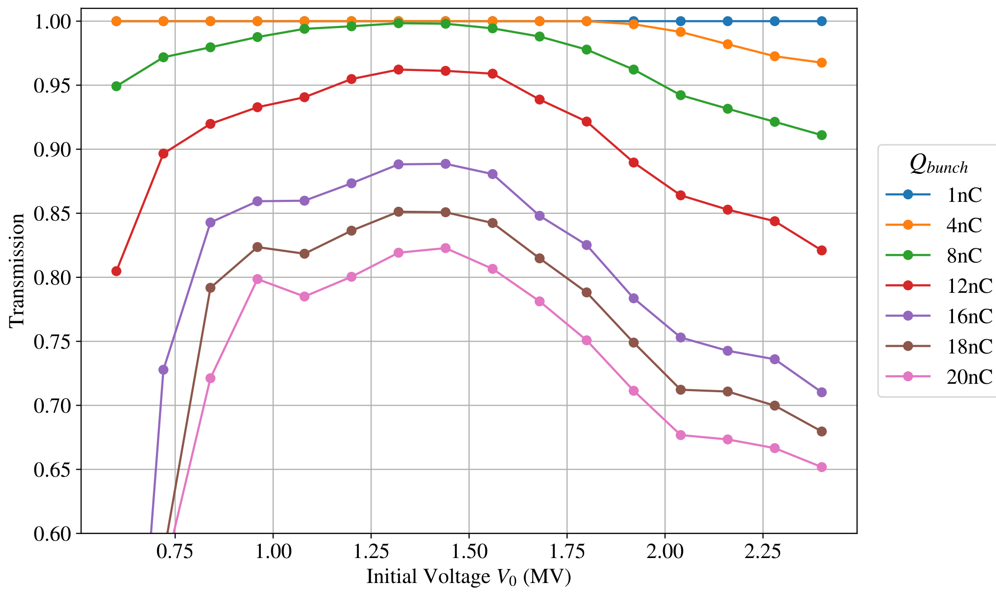

Figure 6: Transmission vs. initial voltage V_0 for various bunch charges

4.1.3 Detuning and Beam Loading

At low charge, one expects detuning Δf to play a small role, both because the transmission is quite insensitive to parameter changes when $Q_{bunch} < 10$nC, and because beam loading has a relatively small effect. However, at higher charges, beam loading begins to become significant, especially at the current coupling coefficient $\beta = 1$. As coupling increases to $\beta = 3$, we expect the impact of detuning to decrease.

With `elegant` simulations, we confirm these general trends (Figure 7). For $\beta = 1$, detuning can have a clear beneficial effect for transmission, enabling a transmission increase of up to 5% (especially at high charge). Moreover, there is a well-defined relationship between detuning and transmission, with an optimal value of detuning (occuring somewhere around $\Delta f \approx -3$kHz). However, in the $\beta = 3$ case, there is little to no correlation between detuning and transmission. Even allowing for a statistically significant relationship, simulation results indicate that the increase in transmission brought by adjusting detuning is marginal at best, with a difference of at most 2%.

4.1.4 PAR Bunch Shortening

The importance of bunch length was briefly explored in §4.1. A large initial bunch length σ_s proves to be the largest source of losses. Significant parts of the beam simply fall out of the RF bucket within the first 200MeV, due to the increased momentum spread that a high initial bunch length eventually brings about. Therefore the improvements brought by a reduced initial bunch length are quite significant, comparable in magnitude to those made possibly by adjusting V_0. Paired with the optimal initial voltage $V_0 = 1.47$MV, this reduction in σ_s suggests that requirement (I) is feasible in the APS-U: at an injected charge of 20nC, we have just over 18nC of output (Figure 8).

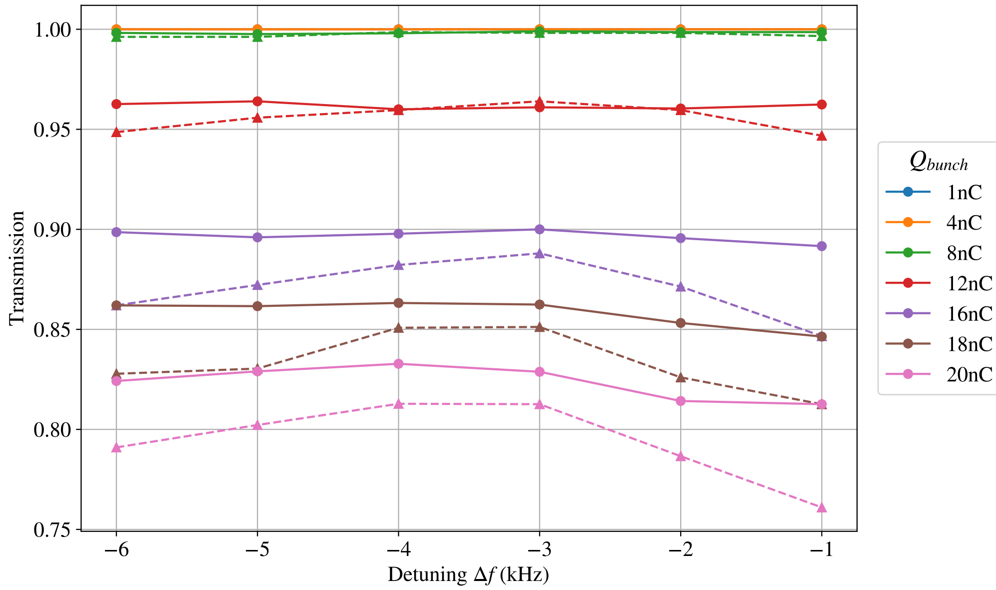

Figure 7: Transmission vs. RF detuning Δf for various bunch charges. Each detuning configuration was run twice, one for $\beta = 1$ (marked with dashed lines and ▲ markers), and one for $\beta = 3$ (marked with solid lines and ● markers).

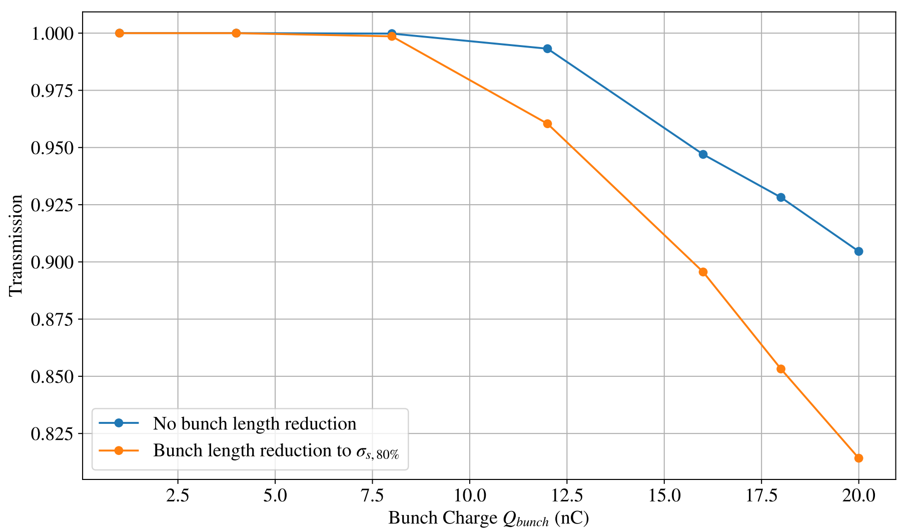

Figure 8: Transmission vs. bunch charge with increased PAR longitudinal focusing on and off. Both were run with the standard reference parameter configuration.

4.2 Momentum Offset Excursions

A noteworthy effect (separate from transmission studies) was the large initial oscillation in the *average* momentum offset $\langle\delta_p\rangle$.

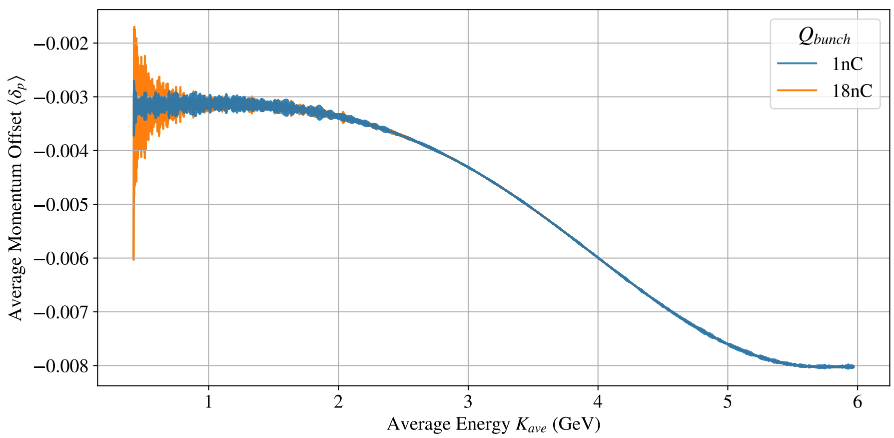

Figure 9: Average momentum offset $\langle\delta_p\rangle$ for an injection charge of 1nC and 18nC

This effect is again due to increased beam loading at high charge. It appears to be independent of the previously discussed parameters, appearing in all configurations. It was hypothesized that injecting the beam at a slight offset in time would mitigate the amplitude of these initial excursions. We first define a metric called the excursion amplitude Δ as the difference between the maximum $\langle\delta_p\rangle$ and minimum $\langle\delta_p\rangle$ for the first 200 turns. There is a clear relationship between $\delta_{t,0}$ and excursion amplitude (Figure 10): a minimum exists for each bunch charge, and this minimum appears to shift further to the left as charge increases. Furthermore, for lower charges, there appears to be some benefit to injecting off in time. However, the gradually flattening curves for high charge seem to indicate that there is little that can be done about these large initial oscillations: the minimum for $Q_{bunch} = 20$nC only fares better than the default $\delta_{t,0} = 0$ by a marginal amount in terms of excursion amplitude. Furthermore, at high charge, there appears to be no statistically significant relationship between transmission and initial time offset. It is quite possible that these large oscillations will pose a problem in practice, and different techniques must be employed to address this.

4.3 Extraction Emittances and Bunch Length

With regards to emittance and bunch length at extraction, we can now fix the initial voltage to be the simulated optimum $V_0 = 1.47$MV. With this, it was found that the horizontal emittance ϵ_x curves were virtually indistinguishable for any combination of parameters. Even with different initial momentum offset $\delta_{p,0}$, the curves remained identical, indicating that ϵ_x is relatively insensitive to different frequency ramps. The horizontal emittance at extraction was 55nm. On the other hand, bunch length σ_s showed some variation with different configurations. However, the behavior towards the end of the momentum ramp was again identical for all configurations. This similar behavior holds even when the initial bunch length is the reduced $\sigma_{s,80\%}$ (Figure 11).

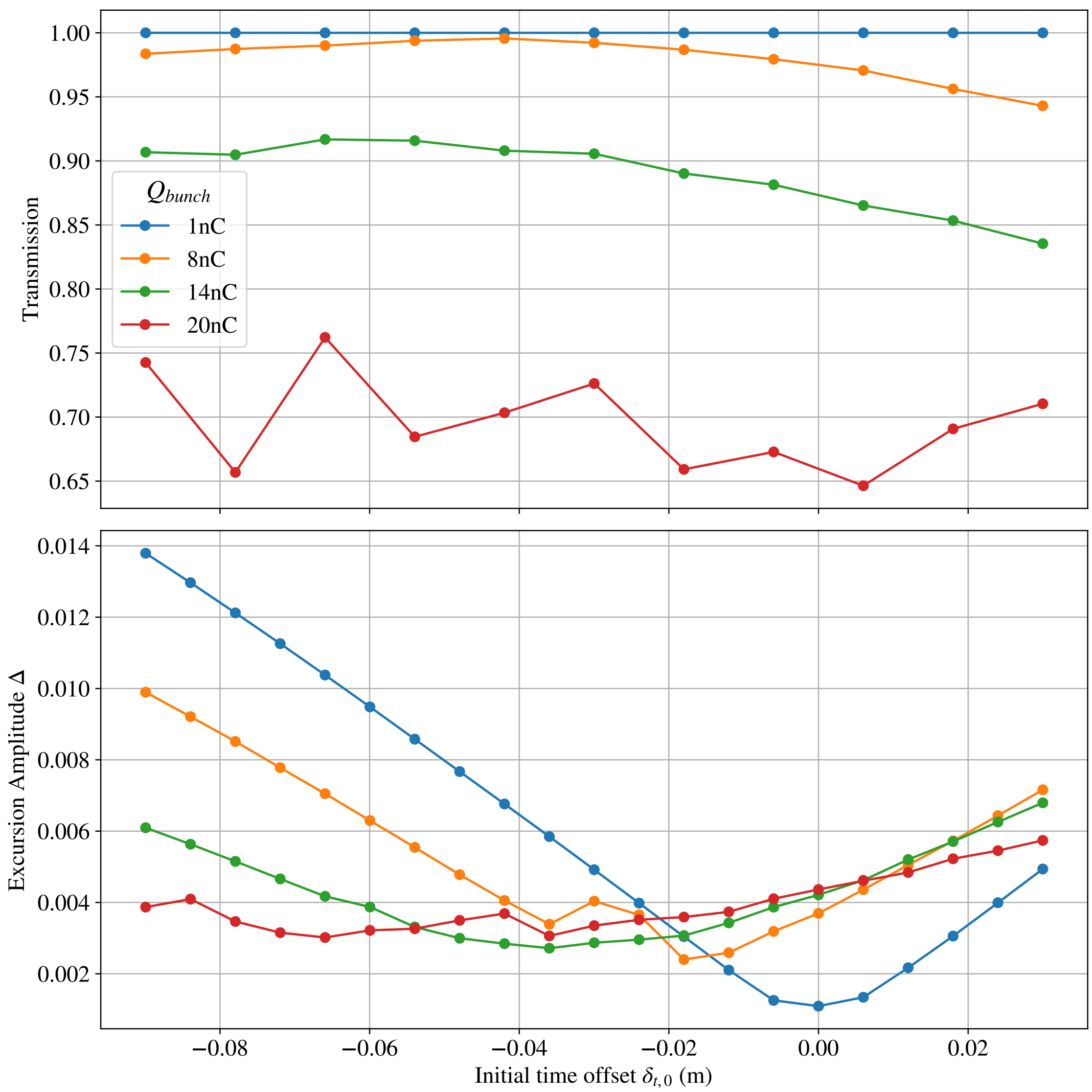

Figure 10: Injecting the beam at various time offsets $\delta_{t,0}$, and the effect on excursion amplitude Δ and transmission at 600MeV.

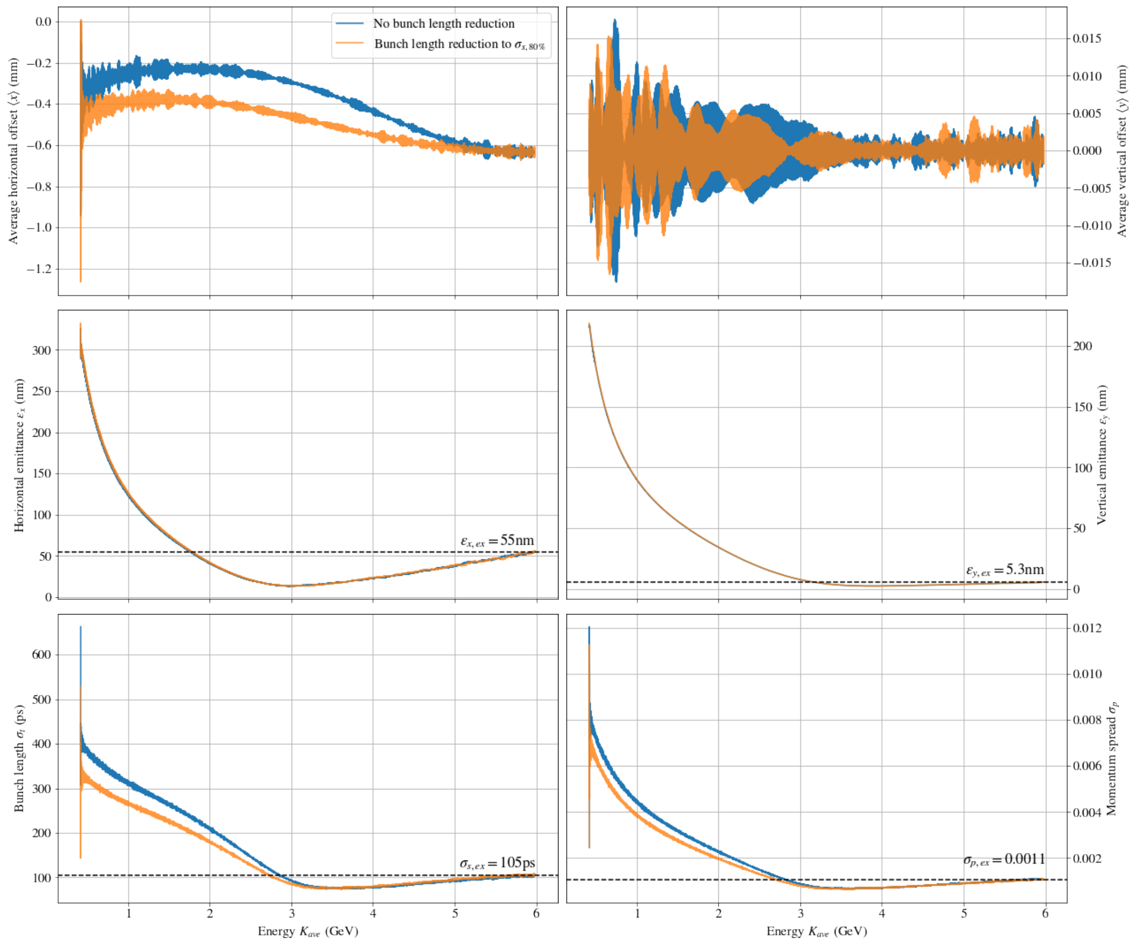

Figure 11: Beam statistics for $Q_{bunch} = 18$nC with bunch length reduction on and off

Now, since the behavior towards the end of the ramp for emittance and bunch length are remarkably similar over all parameter configurations, for the purposes of this study, we can speak of *the* extraction emittance and bunch length for each bunch charge (Table 2). In current simulations, regardless of bunch charge, the horizontal emittance satisfies requirement (II) and stays below < 60nm.

Table 2: Beam Parameters at Extraction

Parameter	Value at Extraction
ϵ_x	55nm
ϵ_y	5.3nm
σ_s	105ps
σ_p	0.0011

5 Future Work

The results presented in this report are promising towards the prospect of delivering high charge from the APS-U booster. However, as noted previously, some techniques employed may have been overly optimistic about beam transmission. More specifically, two assumptions were made about the booster ring that must be further investigated.

1. The booster lattice was approximated as a singular matrix element, and therefore effects not modelled by `ILMATRIX` were not included. This includes physical apertures that may have caused losses from a horizontal emittance ϵ_x that grew too large. This may be solved by using element-by-element tracking, which may be significantly more computationally expensive, however, it will give us a more accurate picture of booster losses.

2. The booster momentum acceptance was taken to be $\pm 2.5\%$, which remains to be verified with further studies.

Furthermore, the large momentum offset excursions at high charge discussed in §4.2 are not a desirable effect. Different techniques may be tried in the future to mitigate the magnitude of these excursions.

Acknowledgements

I would like to express my sincerest gratitude for the guidance and mentorship of U. Wienands and J. Calvey over the course of this project. Work was supported by the U.S. Department of Energy, Office of Science, Office of Nuclear Physics, under contract DE-AC02-06CH11357.

References

[1] J. Calvey, T. Berenc, and K. Harkay. Plan for operating the booster cavities with static tuners in the aps upgrade. Technical Report AOP-TN-2018-074, Advanced Photon Source, September 2018.

[2] J. Calvey et al. Simulations of booster injection efficiency for the aps-upgrade. Technical Report WEA1CO03, October 2016.

[3] J. Calvey. Simulations of booster injection efficiency. Technical Report OAG-TN-2018-041, Accelerator Division, Advanced Photon Source, July 2018.

[4] U. Wienands APS-U Injector Timing and Synchronization. BTC Software Specification Document APSU_2039454, May 2020.

[5] J. Calvey. Booster rf gap voltage requirement for the aps-upgrade. Technical Report OAG-TN-2018-028, Accelerator Division, Advanced Photon Source, April 2018.

[6] J. Calvey. Simulation of Beam Parameters over a Full Booster Ramp. Technical Report AOP-TN-2020-035, Accelerator Division, Advanced Photon Source, May 2020.